Structural model updating of the Gageocho Ocean Research Station using mass reallocation method

Byungmo Kim [1a] and Jin-Hak Yi[*1,2]

[1] *Department of Convergence Study on the Ocean Science and Technology, Ocean Science and Technology School,*
Korea Maritime and Ocean University, Busan, South Korea
[2] *Coastal Development and Ocean Energy Research Center, Korea Institute of Ocean Science and Technology, Busan, South Korea*

Abstract. To study oceanic and meteorological problems related to climate change, Korea has been operating several ocean research stations (ORSs). In 2011, the Gageocho ORS was attacked by Typhoon Muifa, and its structural members and several observation devices were severely damaged. After this event, the Gageocho ORS was rehabilitated with 5 m height to account for 100-yr extreme wave height, and the vibration measurement system was equipped to monitor the structural vibrational characteristics including natural frequencies and modal damping ratios. In this study, a mass reallocation method is presented for structural model updating of the Gageocho ORS based on the experimentally identified natural frequencies. A preliminary finite element (FE) model was constructed based on design drawings, and several of the candidate baseline FE models were manually built, taking into account the different structural conditions such as corroded thickness. Among these candidate baseline FE models, the most reasonable baseline FE model was selected by comparing the differences between the identified and calculated natural frequencies; the most suitable baseline FE model was updated based on the identified modal properties, and by using the pattern search method, which is one of direct search optimization methods. The mass reallocation method is newly proposed as a means to determine the equivalent mass quantities along the height and in a floor. It was found that the natural frequencies calculated based on the updated FE model was very close to the identified natural frequencies. In conclusion, it is expected that these results, which were obtained by updating a baseline FE model, can be useful for establishing the reference database for jacket-type offshore structures, and assessing the structural integrity of the Gageocho ORS.

Keywords: Gageocho Ocean Research Station; jacket-type offshore structure; model updating; mass reallocation method; pattern search

1. Introduction

Ocean research stations (ORSs) play important roles as comprehensive oceanography laboratories that support diverse research ranging from long-term observations of marine physics, climates, environments, and marine biology, to typhoon and particulate matter tracking. There are three ORSs in operation in Korea, including the Ieodo, Gageocho, and Sochengcho ORSs that were respectively established in 2003, 2009, and 2014. They are located in the Yellow Sea between China and Korea (see Fig. 1), because a wide variety of ocean and meteorological phenomena occur in these waters, such as typhoons and the transportation of particulate matter. The structural integrity of the ORS structures must be maintained to ensure that they remain stable during their design lifetime. However, in 2011, Typhoon Muifa critically damaged the Gageocho ORS; consequently, numerous components, such as data transmission cables and a diesel generator, were broken. A long time and extensive effort were required to rehabilitate

them and enhance the overall structural integrity such that the ORS could resume normal operation. Fig. 2(a) presents the Gageocho ORS before and after the damage in 2011 (Shim *et al.* 2015, Kim *et al.* 2017). The most significant structural modification was the heightening of the superstructure (i.e., up to 5 m) as seen in Fig. 2(b) (Woo and Sin 2012, Kim *et al.* 2019), which was purposed to increase the clearance of the platform and thus prevent excessive uplifting owing to the force of abnormally high waves. For this purpose, four steel tubular members were newly fabricated and inserted between the superstructure and substructure of the Gageocho ORS. The diameter and thickness of the new members were larger than those of the existing members to ensure that the structural strength would be higher. To prevent such an accident from recurring after the reconstruction, a structural vibration monitoring system was implemented by installing sensors onto the Gageocho ORS for structural health monitoring (SHM); this was as one of measurement-based preventative maintenance ways.

SHM has been developed in various fields ranging from bridges to buildings to guarantee structural safety by real-time or quasi-real-time monitoring. Compared to such the usual architectures, however, there are several distinctive things in offshore jacket structures. Above all, the general

---

Fig. 1 Locations of operational ORSs in South Korea

buildings are designed to be maintained for a long time up to more than a hundred years. In contrast, the lifetime of the offshore structures is much shorter, e.g., usually for about 30 years, which means that the offshore construction market tends to flourish along with such the period. However, the market is also greatly affected by oil prices and the worldwide industrial boom. Therefore, re- or up-cycling of an offshore structure can be an efficient alternative during low oil price ages like these days. It was reported, for instance, that about 98% of materials comprised of the substructure, accommodation module, and helideck of the North West Hutton platform were recycled or reused. Not only that, nearly 100% of steel materials of DP1, DP2, and QP jackets were recycled, as well (Oil & Gas UK 2012). As a result, SHM, combined with model updating, would be one of the important ways not only to ensure safety but also to reduce capital costs in the offshore field.
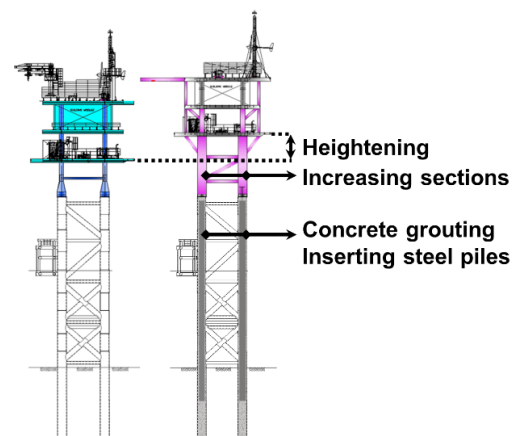
There are two approaches for SHM (Cremona and Santos 2018). The first approach is forward-type, and the

second approach is inverse-type. The former entails only using measured data for the evaluation of structural safety, whereas the latter entails utilizing a simulation model (hereafter referred to as the baseline model), such as a finite element (FE) model, in combination with sensing data; this approach is more common than the forward method. To further explain, the structural characteristics derived from measurements are compared to those derived from the baseline model; then, the cause of the differences between them are analyzed to assess the damage and current structural state. These are the processes of the general inverse SHM. Therefore, the most essential prerequisite for precise SHM is the establishment of an accurate baseline model, which is hereafter referred to as a model updating. Thus, the updating process shall be conducted in consideration of the structural characteristics that will be monitored in the next SHM cycle. Various features that reflect the structural states, such as static displacement, response to impact, or dynamic response, can be applied to SHM. Among these structural states, it is most common to utilize the vibrational characteristics, i.e., the natural frequencies and mode shapes, to monitor structural integrity (Fritzen *et al.* 2013). This is because they can be continuously analyzed based on measured dynamic responses without the information on excitation force which are very difficult or impossible to measure.

In the case of the Gageocho ORS, the dynamic properties were also investigated by using the measured responses to analyze the structural system (Kim *et al.* 2017). As an engineering background of this paper, the SHM system of the Gageocho ORS introduced in the precedent study (Kim *et al.* 2017) was briefly summarized herein. Firstly, the sensor system consisted of accelerometers and tiltmeters installed as shown in Fig. 3 with a sampling frequency of 100 Hz. Table 1 shows the specification of the sensors. Secondly, the data measured during the several days when the significant wave height and mean wind speed were relatively large were collected since the data acquired under such the environmental condition were likely high quality and more suitable for experimental model identification. Thirdly, the measurement data were analyzed by LS-FDD method
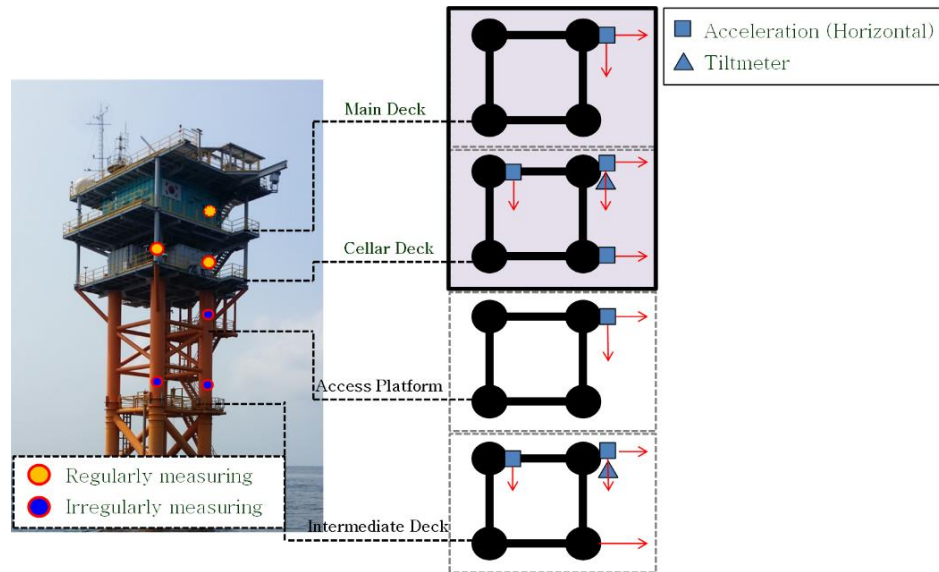

(a) Photo (Shim *et al.* 2015, Kim *et al.* 2017)   (b) Main changes to the structure (Woo and Sin 2012, Kim *et al.* 2019)

Fig. 2 Gageocho ORS before and after recovery

Fig. 3 Dynamic response measuring system of Gageocho ORS (Kim *et al.* 2017)

Table 1 Installed sensors on Gageocho ORS (Kim *et al.* 2017)

Sensor	Model (Manufacturer)	Measuring range	Set	Location	Unit	Indicator
Accelerometer	2220-002 (Silicon Designs Inc.)	±2g	2	Main deck	m/s²	🟦
			4	Cellar deck		
			2	Access platform		
			4	Intermediate deck		
Tiltmeter	SCA121T-D07 (Murata Electronics)	±30°	1	Cellar deck	deg	🔺
			1	Intermediate deck		

proposed by Yi *et al.* (2013), and as a result, the mode shapes were obtained as shown in Fig. 4, and the natural frequencies were evaluated, as well. It was reported that the natural frequencies slightly varied by hour within the range of three decimal places in Hz, assumedly because of the

influence of the environmental variation, such as the temperature and tidal level (Kim *et al.* 2006). As follow-up research and as the first step of SHM to facilitate maintenance of the Gageocho ORS, a baseline model of the Gageocho ORS that accurately simulates the natural

(a) 1st mode (1st bending mode in weak axis) (b) 2nd mode (1st bending mode in strong axis) (c) 3rd mode (1st torsional mode) (d) 4th mode (2nd bending mode in weak axis) (e) 5th mode (2nd bending mode in strong axis)
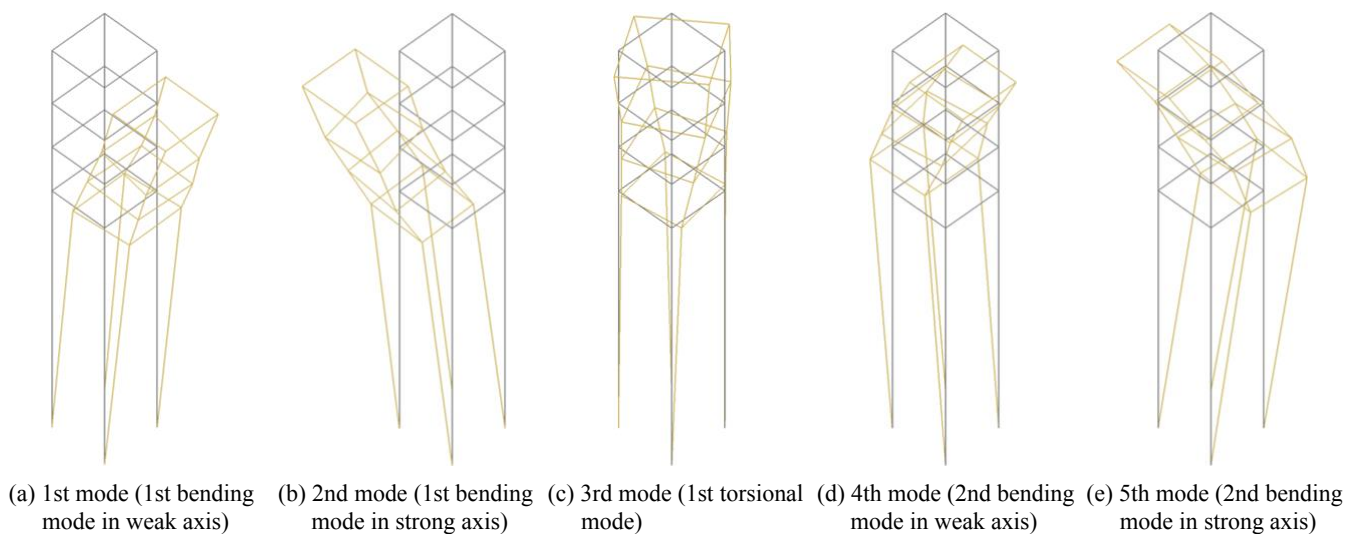
Fig. 4 Mode shapes of Gageocho ORS

frequencies identified during previous studies was developed in this study. In particular, the averages of the measured natural frequencies were regarded as the reference natural frequencies of the Gageocho ORS in this study.

As methodological background and from a fundamental point of view, three dynamic characteristics, frequency response functions (FRFs), mode shapes, and natural frequencies, can be a comparison point of the model updating (Sehgal and Kumar 2015). For instance, the FE model updating was conducted on the Canton tower, a skyscraper. At first, the modal parameters, i.e., the natural frequencies and the mode shapes of the building, were experimentally investigated, and a suitable simplified FE model was established (Ni *et al*. 2012). The FE model was updated based on the modal parameters by a direct matrix updating method (Lei *et al*. 2012). Besides, there is an example that the FRFs with natural frequencies were used to update an FE model of a reinforced concrete structure with the aim of seismic damage detection (Yu and Chung 2012). Regarding the Gageocho ORS, at first, the FRFs would be difficult to be applied. This is because it is basically the ratio of harmonic response to the harmonic excitation force (Sehgal and Kumar 2015), whereas the excitation forces on the ORS are very complicated, such as waves, wind, and currents, derived from Mother Nature. At second, it might be possible to utilize various techniques based on similarity of the mode shapes, such as Modal Scale Factor (MSF), Modal Assurance Criterion (MAC), and Coordinate MAC (COMAC), for the model updating in virtue of the preceding paper on the Gageocho ORS (Kim *et al*. 2017). However, not only the limited number of sensors attached to the ORS but the measurement only focusing on the upper range of the structure owing to the submerged parts, are likely to bring about incorrectness in the FE model updating. For these reasons, the natural frequencies are used in this research.

In the case of offshore structures, on the other hand, there are only some relevant references. Li and Li (2011) carried out research to update the boundary condition of an offshore jacket structure using the cross model cross mode (CMCM) method based on numerical simulations. Hosseinlou *et al*. (2017) applied the CMCM method to develop a structural integrity monitoring process for a jacket structure and validated it with a plane frame structure in laboratory tests. Hosseinlou and Mojtahedi (2016) proposed an effective way to update the FE model focusing on lessening the side effect of FE model reduction based on incomplete measurements and proved it using a 3D jacket model in a laboratory experiment. However, references for a real offshore structure in operation are rare. Presumably, the reason for this is that most offshore structures are owned by oil and gas companies so detail information of the real structures is likely to be confidential. Therefore, this study aims not only at modeling the FE model most well-matched to the measured natural frequencies of a real offshore structure in operation, i.e., the Gageocho ORS herein, but also at reporting the entire procedure of model updating from comparison of the natural frequencies to estimation of error sources, summary of relevant references, establish-

ment of the strategies for model updating because it is worthy of sharing as an example of updating an FE model of an offshore jacket structure in field operations.

2. Approach to model updating

2.1 Preliminary simulation model and the result comparison with measured data

2.1.1 Description of preliminary simulation model

As with all other offshore structures, the preliminary numerical modeling and safety check for the Gageocho ORS were performed before the retrofit construction (Woo and Sin 2012). In this study, the original model that was constructed by using a commercial offshore analysis program SACS (Engineering Dynamics, Inc. 1995) was transformed into an FE model by using a commercial FE analysis program ANSYS Mechanical APDL (ANSYS, Inc. 2017). In details, all members were identically modelled with the design of the ORS so the preliminary model has the same topology with the structure. The added mass which is the hydrodynamic effect proportional to the acceleration of an object in a fluid, was considered as well. In terms of the boundary condition, the nodes of the four jacket legs, which are connected to the seabed, were fixed for the six degree of freedom. However, the ultimate purpose of the design report was to verify the structural strength against the environmental loads so the model were conservatively made. For instance, the steel piles in the jacket legs and concrete grouting were not modeled, and the sizes of the member sections were also conservatively applied under the assumption of full erosion. All additional masses but for the steel jacket structure itself were regarded as weight instead of increasing the density of the jacket structure to 5% ~10%. All these settings were according to the design report (Woo and Sin 2012).

2.1.2 Comparison with measured data and the results from the preliminary model

Generally, there is a certain level of uncertainty and modeling error in the structural analysis model; thus, the results of the model simulation tend to disagree with the measured responses for the target structure. In the case of the Gageocho ORS, the calculated natural frequencies for the lowest five modes obtained from the preliminary FE model were much larger than the identified natural frequencies obtained via the measured responses, as shown in Table 2. Hence, it is vital to accurately update the FE model for successful SHM. The 1st and 2nd modes correspond to the 1st bending mode in two perpendicular directions, the 3rd mode is the 1st torsional mode of the Gageocho ORS, and the 4th and 5th modes correspond to the 2nd bending mode in the perpendicular directions. The difference between the two natural frequencies corresponding to the same mode type was calculated by dividing the difference by the mean value of both. For example, the difference of the measured natural frequencies for the 1st bending mode is 2.05% computed by 100 × (1.827–1.790)/{(1.827+1.790)/2} much larger than 0.14%

Table 2 Natural frequencies, as determined by the measurement responses (Kim *et al*. 2017) and preliminary FE model for the Gageocho ORS, and differences between the natural frequencies of same mode types

Mode number	1	2	3	4	5	RMSE
Measurement [Hz]	1.790	1.827	2.652	5.599	5.694	-
Preliminary model [Hz]	2.212	2.215	3.098	6.132	6.260	-
Error [%]	23.58	21.24	16.82	9.52	9.94	17.20
Mode type	1st bending		1st torsion	2nd bending		-
Difference [%] Measurement	2.05		-	1.68		-
Preliminary model	0.14		-	2.07		-

which is the corresponding value of the preliminary model. This would mean that there is a factor in the Gageocho ORS, inducing the eccentricity but not included in the preliminary model, such as mass distribution. It is also notable that the tendency of the differences for the 1st and 2nd bending mode are entirely dissimilar each other in the case of the measurement and the preliminary model. For instance, the difference between the measured natural frequencies for the 1st bending mode is 2.05%, which is much larger than 0.14%, which is the corresponding difference for the preliminary model, as mentioned before. Between the measured natural frequencies for the 2nd bending mode, on the contrary, the difference of 1.68% is less than the corresponding difference of 2.07% for the preliminary model. This observation would be interpreted as that the cause of the eccentricity makes influence differently on the 1st and 2nd bending mode.

2.2 Root cause analysis for the errors in design and construction

The causes for these errors were scrutinized to make the simulation model compatible with the measured result. Relevant with this matter, Mottershead *et al*. (2011) comprehensively categorized possible errors and causes in model updating into three types: (1) Idealization errors on a physical structure; (2) Discretization errors of a FE model; (3) Errors of model parameters, and lots of details and examples were briefly stated ranging from material properties, cross-sectional parameters, and non-structural mass as the last category, to boundary conditions, nonlinearities, and simplifications of the structure and mass properties as the first category. Among the considerations in the list, the stiffness distribution and the boundary condition would be most influential not only to the natural frequency and dynamic characteristics of a structure but also to all the general FE problems from the perspective of structural engineering. In a real problem, however, it does not always mean finding the true solution just because theoretically the most sensitive factors are used as the variables to solve the problem. Which physical parameters are controlled or independently dealt with as variables, should be decided based on the real states of the structures as well as just the theoretical basis in order to prevent a wrong solution.

On such the point, the boundary condition was set to rigid in this research. Specifically, four piles as the founda-

tion of the Gageocho ORS were deeply penetrated into the hard rock soil with the massive amounts of the concrete grouting as shown in Fig. 2(b). In addition, there has been no occurrence of geotechnical phenomenon enough to weaken the base, such as a severe earthquake exceeding the design criteria. Last but not least, the field inspection resulted in no significant and progressive tile of the columns (Woo and Sin 2012). All these considerations from the rigidity of the hard bedrock, the deep penetration of the piles, and the huge mass of the grouting to no critical external force and pressure and the straightness of the columns, support the assumption of the rigid bottom boundary condition of the Gageocho FE model.

On the basis of this list except for the boundary condition, in this study, the causes of the above-mentioned errors were investigated in two aspects, the inaccuracy of the simulation model and the uncertainties of the construction process. Regarding the simulation model, the concrete and steel piles that were inserted into lower parts of jacket legs, as indicated in Fig. 2(b), were omitted in the preliminary FE model. Additionally, the sections of the jacket legs in the splash zone were modeled as the most corroded. The reason for this was to ensure that the stiffness values of the main components in the jacket structure were underestimated so as to maximize the stress results for static analysis and ensure a more conservative safety estimation. However, these conditions resulted in highly discrepant dynamic characteristics, because the stiffness was underestimated and the considerable mass of the concrete was not considered.

In addition, only major members of the jacket structure, e.g., jacket legs, braces, and decks, were included in the preliminary model; therefore, the masses of various other components were applied as dead loads. The reason for this may have been to simplify the model for more efficient analysis. However, the total amount of the omitted mass equates to more than 30% of the total mass of the modeled steel structures. Therefore, the dynamic properties, particularly the natural frequencies, which are fundamentally based on the ratio of stiffness to mass, were heavily exaggerated. Moreover, the center of mass cannot be precisely embodied, so the asymmetry between the strong axis and weak axis of the measured natural frequencies shown in Table 2 cannot be quantified.

Lastly, a significant contribution to construction error is the ambiguity of the strength of the concrete materials. To

Table 3 Causes of the discrepancy between the preliminary analysis results and Gageocho ORS measurements

	Reason	Cause
Preliminary simulation model	Conservative safety check	Omission of concrete in jacket legs
		Omission of steel piles in jacket legs
		Modeling sections with the most corroded in splash zone
	Mass simplification	Regarding mass of equipment and other components as dead loads
Construction process	Uncertainty of material properties	Curing of concrete filled with seawater in flooded jacket legs

further explain, the specified compressive strength of concrete (f_{ck}) is assumed to be 28 GPa in the design stage (i.e., before construction), but, in practice, the 210 m³ cement is simply poured into the four jacket legs that are flooded with saline sea water (Woo and Sin 2012). Considering the fact that the material properties of concrete are entirely dependent on the curing process, particularly the water-cement ratio, composition of the cement, temperature, and humidity, utilizing such a method to pour concrete increases the level of uncertainty of its material properties. This uncertainty may be one of the causes of the errors.

2.3 Strategies to build a more realistic FE model

In this study, the Gageocho FE model was updated fully based on the root causes previously investigated, and other usual approaches, such as the distribution of the stiffness over the structure, were not considered. This is because any critical damage to the major members, which can induce the eccentricity of the measured natural frequencies, was not specifically detected and referred to in the field inspection and reconstruction design report (Woo and Sin 2012). Even if there are a few minor errors of the stiffness of the individual member or some region, it would not make a predominant effect on the dynamic characteristics of the ORS, compared to the stiffness of the completely neglected concrete grouting. Moreover, using too many variables, for instance, the stiffness distribution over all the individual jacket leg and brace members, is likely to cause the overfitting of the optimal solution particularly in the case with great uncertainty like this example, even though it is general in optimization that the more variables the better convergence. These are the reason why it is the priority to establish the Gageocho FE model correctly reflecting the actual states of the ORS, rather than to pay attention to other approaches like the stiffness distribution.

2.3.1 Approach of model updating
Among the possible causes that were previously mentioned, it would be relatively easy to correct the disregarded concrete and steel piles, and the corroded areas in the splash zone. However, it is difficult to exactly predict the material properties, such as the mass and stiffness of the concrete, due to uncertainty. Assuming that the legs are not broken, and thus there is no cement leakage, the total mass of the concrete filling in the legs can be considered as constant. Regardless of this assumption, the stiffness of the concrete remains to be unknown.

In addition to the concrete-related error, the equipment and other components listed in Table 4, which were simply regarded as loads in the preliminary FE model, should be considered as masses. This is because, as mentioned earlier, the natural frequency theoretically reflects the ratio of stiffness to mass. More specifically, mass is one of the two fundamental contributions to natural frequency; therefore, a more accurate model of the mass elements would increase the accuracy of the updated simulation model. Moreover, in this case, it is also an important prerequisite for identifying the uncertain stiffness of the concrete. Because the stiffness is expected to have high uncertainty, the mass has to be exactly modeled to correctly find another factor that contributes to the natural frequency, i.e., the unknown stiffness of the concrete. According to the reference report

Table 4 Disregarded mass elements in the preliminary FE model, and their locations

Category	Item	Locations	Approach
Appurtenance	Anode	Brace	Individual modeling
	Grating		
	Handrail		
	Stair		
Equipment	Photovoltaic power generator	Topside decks	Integration & reallocation
	Hoist crane		
	Rainwater service tank		
	Lantern		
	Wind power generator		
	Diesel generator		
	Diesel tank		
Facilities	Buildings		
	Walls		

Table 5 Masses of the Gageocho ORS

		Load [kN]	Mass [ton]
Dead load of the jacket structure		3346.713	341.2
Omitted parts	Appurtenance	650.656	72.9
	Equipment	169.970	17.3
	Facilities	129.380	13.2
	Subtotal	-	103.4

(Woo and Sin 2012), in addition, the total amount of the masses calculated from their loads considering the hydro-static and -dynamic effect is approximately 103.4 ton, and this is almost one-third of the weight of the whole steel jacket structure as seen in Table 5. This objectively lends support to the necessity for consideration of the ignored masses.

However, updating an FE model with controlling mass should be carefully treated although model updating based on the modal parameters allows to deal with stiffness and mass. This is because they fundamentally result from the eigenvalue analysis of a system, i.e., the natural frequencies are a function of the mass and stiffness. Hence, the problem may be indefinite and the optimum may also be totally incorrect if both are used as a variable at the same time. On this matter, one of general ways to reflect the mass is to slightly increase the density of a material but it was already applied to the preliminary model. Therefore, in this study, references for model updating of a real structure considering mass were investigated and enumerated, and then a variety of mass element models were created and compared to determine which is most suitable for the model updating with maintaining the total amount of the masses equivalent to the description in the design report. As long as the authors know, there was no removal or addition of the non-structural masses since design and installation, so the total amounts of the masses would be the same as those of the Gageocho ORS.

2.3.2 Summary of model updating instances inclusive of masses of real structures

In order to appropriately model the masses, similar research papers dealing with the FE model updating of real structures were briefly summarized. Most papers treated concrete bridges (Teughels and Roeck 2004, Fang and Perera 2009, Deng and Cai 2010, Ren and Chen 2010, Han and Luo 2013, Zhou *et al.* 2016). Teughels and Roeck figured out elastic and shear moduli, considering mass as constant concentrated elements. Fang and Perera identified section properties of girders with constant material properties, i.e., density and elastic modulus. While Deng and Cai searched for elastic moduli part by part of a bridge, and a concrete density including additional non-structural masses, Ren and Chen assumed unchanging density and concentrated mass elements to find optimal elastic modulus and areas of connection bearings. Han and Luo also only coped with elastic modulus and horizontal and vertical stiffness of bearing connections as variables in the optimization process while treating mass as just constant density. Zhou *et al.* (2016) considered density as one of the variables together with elastic modulus and stiffness of pears although the optimum density value was not quite different from the design target. It seems that, therefore, the amount and distribution of mass is not a very significant factor for model updating of the bridge-type structure. This would be by reason of the fact that there is seldom mass of non-structural parts on such structures.

Besides, there are other studies on different structural types. Bayraktar *et al.* (2011) researched Dam Berke made of concrete. Young's modulus and density of the Dam itself

and the foundation of it were investigated, and finally, the updated FE model was evaluated under seismic condition. Boscato and Russo (2015) conducted FE model updating for a historical masonry building, Santa Maria del Suffragio church, severely damaged by an earthquake in 2009, and assessed elastic moduli and Poisson's ratios of the structure, part by part. However, the mass of the architecture was dealt with as unchangeable density, and some non-structural masses were just considered as fixed concentrated mass elements. Last but not least, Foti *et al.* (2012) carried out a study on a slender concrete tower called Provincial Administration Building using the first five dynamic modes. The research has some interesting things in several aspects. First of all, the tower is vertically slender like the Gageocho ORS, so they seem to have common dynamic characteristics. For example, the third mode of the tower is the first torsional mode and the other four modes are the first two bending modes for two horizontal axes, which are considerably similar to those of the Gageocho jacket. Also, non-structural masses were importantly considered, so not only the density but forty-four mass elements were treated as variables to be identified. The mass elements were regarded to be placed at four corners on every eleven stories of the tower, and their values were figured out. Table 6 concisely shows the results of all the above eight reference papers including measured natural frequencies, natural frequencies analyzed from their updated FE models, and errors between them up to first seven modes.

2.3.3 Direction of model updating

In the case of jacket platforms like this Gageocho ORS, on the other hand, non-structural masses would be more important than the slender tower. The reason for this is that there would be massive crude oils and a lot of equipment on an offshore jacket platform in general. In addition, almost all the non-structural masses would be placed on a topside platform so the overall dynamic characteristics of a whole jacket structure might be crucially affected by them. Moreover, the masses would vary depending on situations, for instance, off-loading of the stored oils, attachment or detachment of facilities. Therefore, this study mainly tried focusing on how to accurately model the additional masses.

In the Gageocho ORS, the total number of masses exceeded 1000, and these masses were originally modeled as dead loads at their respective locations in the preliminary FE model. Therefore, every mass can be modeled at their own locations. However, they have a very complex distribution. For example, a large number of different mass elements can be applied in the same location. Hence, it is quite inefficient, in the modeling and simulation processes, to individually model all of the masses at their own positions.

For this reason, one equivalent mass was modeled for most of the masses, with the exception of the anodes, which were considered to have an integrated mass center; then, the one equivalent mass was reallocated in various ways. The reason for the exception is that, initially, the braces, i.e., a major structural member, are slender, and the anodes are attached to their centers. This means that the dynamic response of the braces is likely to be predominantly affected

Table 6 Results and errors of model updating in the eight reference studies (NF$_m$: measured natural frequencies [Hz], NF$_o$: eigen frequencies of the updated FE model [Hz], and Error [%])

Reference	Mode	1	2	3	4	5	6	7	RMSE
Teughels & Roeck 2004 Concrete bridge	NF$_m$	3.89	5.02	9.8	10.30	12.67	-	-	
	NF$_o$	3.87	5.03	9.72	10.31	12.52	-	-	
	Error	-0.514	0.199	-0.816	0.097	-1.184	-	-	0.690
Fang & Perera 2009 Concrete bridge	NF$_m$	-	-	-	-	-	-	-	
	NF$_o$	-	-	-	-	-	-	-	
	Error	-4.43	1.71	2.78	-	-	-	-	2.461
Deng & Cai 2010 Concrete bridge	NF$_m$	8.19	11.11	15.79	-	-	-	-	
	NF$_o$	8.19	10.79	16.23	-	-	-	-	
	Error	0	-2.9	2.8	-	-	-	-	2.327
Ren & Chen 2010 Concrete bridge	NF$_m$	3.070	3.352	3.957	4.780	5.650	-	-	
	NF$_o$	3.101	3.188	3.73	4.431	5.173	-	-	
	Error	-1.01	3.13	-5.31	-6.8	-12.18	-	-	6.835
Han & Luo 2013 Concrete bridge	NF$_m$	1.56	1.76	2.34	2.15	2.34	-	-	
	NF$_o$	1.60	1.77	2.34	2.18	2.26	-	-	
	Error	2.56	0.56	0.17	1.37	-3.41	-	-	2.020
Zhou *et al.* 2016 Concrete bridge	NF$_m$	0.691	0.730	0.997	1.406	1.480	1.925	2.350	
	NF$_o$	0.683	0.733	0.953	1.398	1.488	1.948	2.369	
	Error	-1.143	0.356	-4.413	-0.548	0.568	1.216	0.826	2.075
Bayraktar *et al.* 2011 Concrete dam	NF$_m$	2.75	3.41	4.78	5.56	6.03	7.94	8.28	
	NF$_o$	2.55	3.41	4.70	5.48	6.07	7.67	8.19	
	Error	-7.27	0	-1.67	-1.44	0.66	-3.4	-1.09	3.410
Boscato *et al.* 2015 Masonry church	NF$_m$	1.94	2.12	2.54	2.71	2.86	3.15	3.24	
	NF$_o$	1.90	2.12	2.53	2.75	2.97	3.17	3.49	
	Error	-1.90	0.17	-0.29	1.57	3.76	0.57	7.58	2.016
Foti *et al.* 2012 Concrete slender tower	NF$_m$	2.301	2.429	4.187	4.599	5.017	-	-	
	NF$_o$	2.331	2.339	4.473	5.503	5.504	-	-	
	Error	1.304	-3.705	6.831	19.656	9.707	-	-	10.418

by the mass of the anodes. Additionally, the anodes are submerged, so their added mass has to be considered. Therefore, the dynamic characteristics of the braces will be inaccurately predicted if the locations of the anodes are ignored. It is for this reason that the anodes were individually modeled, unlike the other components.

2.4 Problem definition and pattern search method

In this research, updating the preliminary FE model was purposed to establish a model that is able to minimize the discrepancy between the calculated natural frequencies and the identified ones based on measurement, which are presented in Table 2. Therefore, the problem can be defined as an error minimization problem, as described in Eq. (1).

$$\min g = \sqrt{\sum_{i=1}^{5} \left\{ W^i \times \left(\frac{f^i(ST, MS) - f_m^i}{f_m^i} \right) \right\}^2} \quad (1)$$

where g is the objective function, i is the mode number, which ranges from 1 to 5 in this case, W^i, f^i, and f_m^i are the weighting factor, the calculated natural frequencies, and the identified natural frequencies based on measurement for the i-th mode, respectively. The weighting factors were applied as follows: 1 for two first bending modes in weak and strong axes (1st and 2nd natural frequencies), 0.5 for the first torsional mode (3rd natural frequency), and 0.25 for two second bending modes in weak and strong axes (4th and 5th natural frequencies). ST and MS are the parameters representing the stiffness and mass of the system respectively, which means that the natural frequency f^i is basically a function of the elastic moduli of the concrete and steel, as well as other parameters, depending on how the integrated mass is reallocated. Thus, it is reasonable that the respective moduli of elasticity of the concrete and steel are taken into account as updating parameters in the model updating.

However, the elastic modulus can theoretically range from 0 to infinity, so it is difficult to define the upper limit

of its domain. Furthermore, as stated previously, it is difficult to accurately determine the value for concrete, meaning that a high computational cost would be required to find its global optimum. In such cases, normalizing methods can be applied to address the matters, for example, min-max scaling and standard score. To decide which way is adequate, the ranges not only of the stiffness parameters but of the other variables shall be considered. The other variables are bounded much narrower than the stiffness variables, which are related to the location of the ignored masses and will be defined afterward in detail. Therefore, the parameter θ, the tangent of which is equal to the normalized value of the elastic modulus, was introduced in this study (Eq. (2)).

$$\tan \theta = \frac{ST - \mu_{ST}}{\sigma_{ST}} \left(arctan \frac{-\sigma_{ST}}{\mu_{ST}} \leq \theta < \frac{\pi}{2} \right) \qquad (2)$$

where ST is an arbitrary unknown variable, particularly for the stiffness of a system, such as the elastic moduli or spring constants, and μ_{ST} and σ_{ST} are the mean value and standard deviation of the variable ST, respectively. Regarding the mean, the elastic modulus values for the steel and concrete materials were assumed to be 200 GPa (E_s) and 27.7 GPa (E_c), respectively (Woo and Sin 2012), in the design stage. For the standard deviation of the steel, a coefficient of variation (COV) of 0.06 was applied (Hess *et al.* 2002). However, the COV of the specified compressive strength of concrete (f_{ck}), which is the main factor affecting the tangential elastic modulus of concrete, has been reported to range between 0.04 and 0.2 (Baji 2014). Considering the imperfect and unclear concrete curing conditions, the largest value of 0.2 was used as the COV of concrete in this study.

Additionally, the pattern search (PS) method, which is one of global optimization techniques, was utilized to obtain the optimum solution of the updating problem described by Eq. (1). Specifically, the PS method directly searches for the optimum by iterating in steps, without utilizing the derivative information of an objective function, as follows: (1) a mesh comprised of points with the same pattern, e.g., the same equidistance from the current searching point, are set in variable space, (2) the values of the objective function for the points are calculated, and (3) the current point moves to the best (i.e., an optimal) point on the mesh if the objective function is less at the best point than at the current point; otherwise, a new mesh is generated with a shrinking pattern at the current point. Fig. 5 (Jacquenot 2009) displays an example of the convergence process of the PS method.

3. Mass modeling cases

3.1 Strategies for mass modeling and additional updating parameters

The equivalent mass (M_T) of the ignored mass elements, and the location of the center ($\vec{c}_T$), are listed in Table 7. The total mass was approximately 90.49 ton, and it was eccentrically placed on the X-Y plane. The height of the center of mass was approximately 24.28 m, corresponding to the distance between the cellar deck and main deck (1st and 2nd floor decks, respectively), as shown in Fig. 6. It should be noted that the heights of the three decks, i.e., the cellar, main, and roof decks, were as 22 m (Z_1), 26.5 m (Z_2), and 31 m (Z_3), respectively. The next step was determining how to embody the integrated mass in the FE model. This step is very important, as the natural frequencies calculated from the FE model are predominantly affected by how the integrated mass is applied. Furthermore, with the exception of the elastic moduli, updating variables are decided by the strategy of modelling the equivalent mass; therefore, the effectiveness
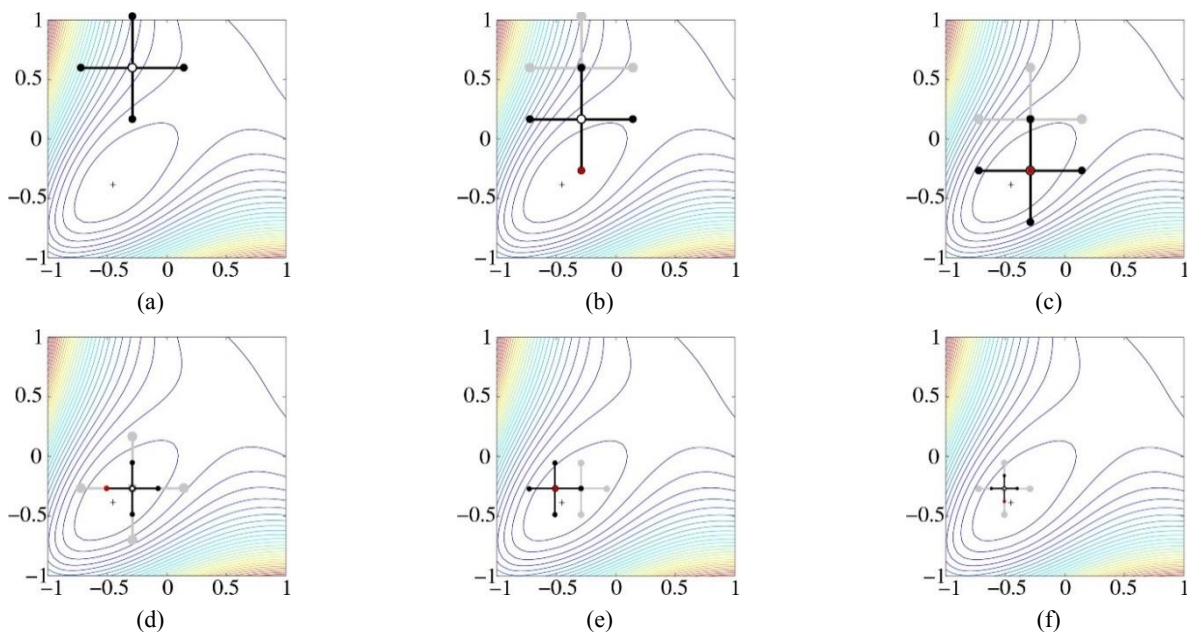

Fig. 5 Example of the convergence process of the PS method (Jacquenot 2009)

Table 7 Equivalent mass and its location

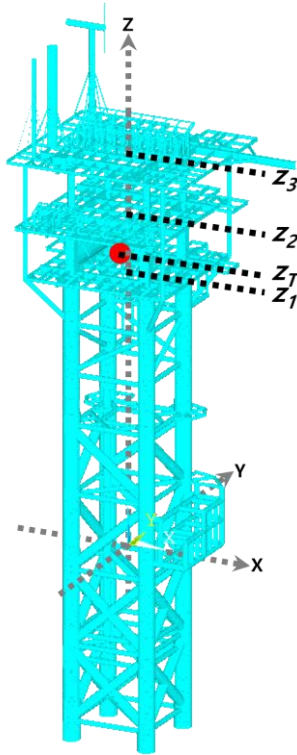| Mass	Center of mass ($\vec{c}_T$)		
M_T [ton]	X_T [m]	Y_T [m]	Z_T [m]
90.491	0.040	0.765	24.278

Fig. 6 Locations of the equivalent mass on the Gageocho ORS

of the model updating is also contingent on it. For these reasons, various strategies were applied, as described in Table 8 and Fig. 7.

3.2 Model 1: distributed mass elements

As illustrated in Fig. 7(a), all dead loads were modeled as nodal mass elements. In the design report by Woo and Sin (2012), it is stated that some of the dead loads were modeled as a single load, whereas the others were modeled as distributed loads; therefore, the distributed loads were transformed into several nodal mass elements. Consequently, 1,569 dead loads were modeled as a total of 3,083 nodal mass elements in this study. This task is generally

highly complex and very time-consuming, so it was essential that it be very carefully performed. Considering the fact that the Gageocho ORS is a relatively small-scale and lightweight offshore structure, as compared to typical commercial offshore jackets in the oil and gas industries, it may be extremely difficult to apply this method to jacket structures that are much larger and more complex than the Gageocho ORS.

3.3 Model 2: equivalent mass with four rigid connections

As shown in Fig. 7(b), the integrated mass was rigidly linked to the closest node on each jacket leg. This can be considered as the most intuitive method, but the excessive stiffness resulting from the rigid connections may distort its dynamic characteristics.

3.4 Model 3: equivalent mass with four spring connections

As described in Fig. 7(c), uniaxial spring elements were used instead of the rigid connections, so their stiffness values were considered to be updating parameters. Unlike the steel members, the tensioners and compensators link components with stiffness; however, the spring connection elements do not actually exist. This means that the mechanical properties of physically nonexistent components have to be determined. Thus, this approach is likely to be somewhat controversial. Regardless of whether the assumption is practically reasonable, these variables contribute to the overall stiffness, so they were parameterized like the elastic modulus E_s, as shown in Eq. (2).

3.5 Model 4: reallocation of masses on upper jacket legs and deck nodes

As seen in Fig. 7(d), the integrated mass was reallocated to form two groups, with 12 nodes on the jacket legs, and two nodes on the decks. It should be noted that the nodal mass elements in the first group were redistributed across 12 nodes to represent the effects of mass distribution along the height of the structure, where the three deck planes intersect the four leg columns at right angles, because most mass elements were originally located on the three decks, as shown in Fig. 7(a). Conversely, the elements in the second group were purposed to explicitly describe the eccentricity on the X-Y plane of the equivalent mass, so they were modeled on the deck planes.

Table 8 Strategies to model the equivalent mass

	Approach	Updating variables
1	Distributed mass elements	E_s, E_c
2	Equivalent mass with 4 rigid connections	E_s, E_c
3	Equivalent mass with 4 spring connections	E_s, E_c, S_1, S_2, S_3, S_4
4	Reallocation of masses on upper legs and deck nodes	E_s, E_c, α, β
5	Reallocation of masses on lower legs, upper legs and deck node	E_s, E_c, α, β, γ

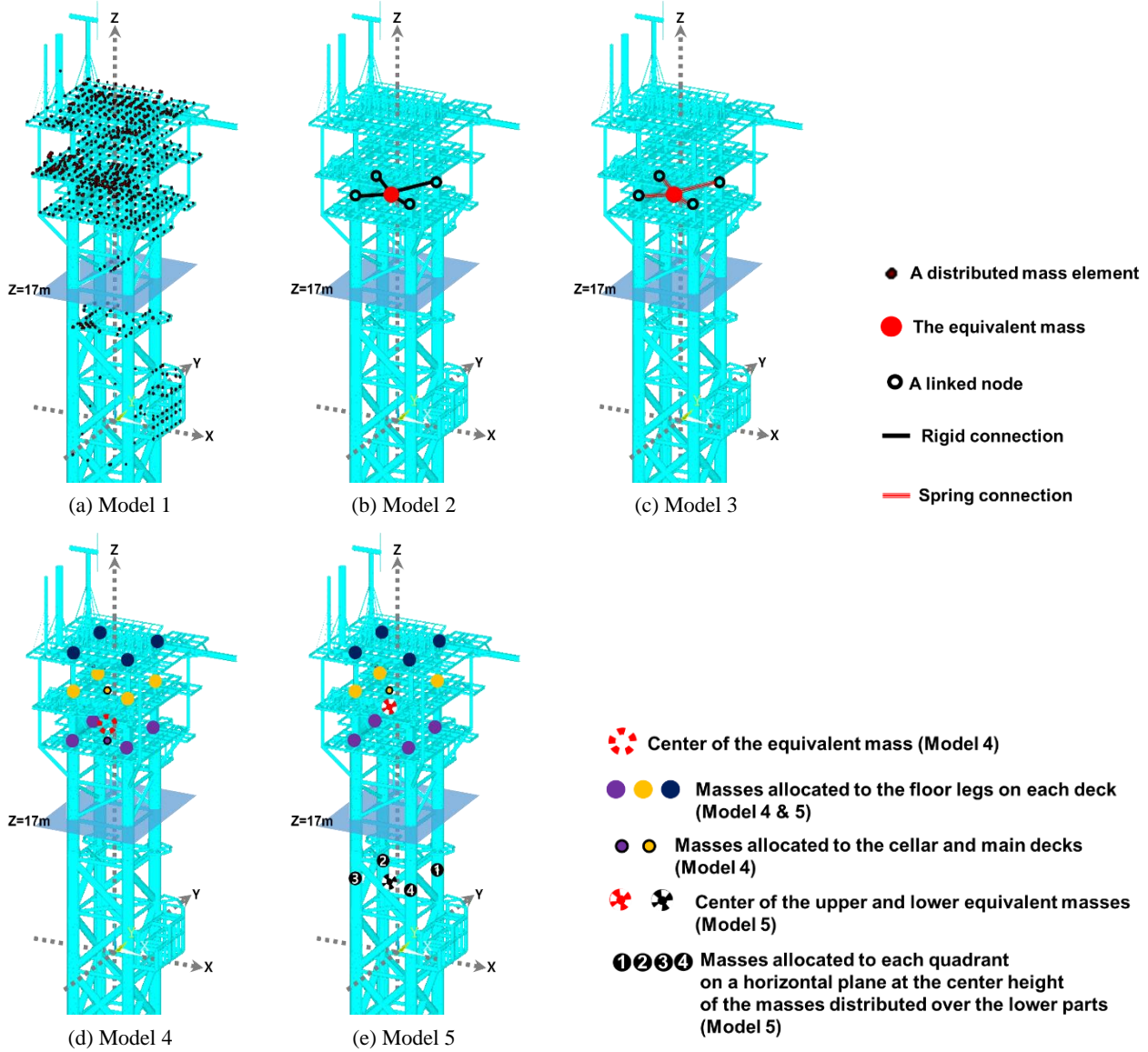(a) Model 1   (b) Model 2   (c) Model 3

(d) Model 4   (e) Model 5

Fig. 7 Initial models based on the five strategies for the disregarded masses

The most important factor is the total mass (M_T); additionally, the center of mass ($\vec{c}_T$) had to be maintained before and after the reallocation, as described by Eqs. (3)-(4).

$$M_T = M_V + M_P \tag{3}$$

$$M_T \cdot \vec{c}_T = M_V \cdot \vec{c}_V + M_P \cdot \vec{c}_P \tag{4}$$

where M_V and M_P are the total masses applied to the 12 leg nodes and two deck nodes, respectively. $\vec{c}_V$ and $\vec{c}_P$ correspond to the centers of M_V and M_P, respectively. M_V was divided into M_{V1} on the 1st floor, M_{V2} on the 2nd floor, and M_{V3} on the 3rd floor, and the four intersection nodes on each deck shared equal portions of the mass, as shown in Fig. 8(a). This means that the centers of M_{V1}, M_{V2}, and M_{V3} were always located at the origin of the X-Y plane, along with $\vec{c}_V$. Consequently, the only variable that was able to represent the horizontal effect of the center of mass was M_P, so the roles of the two mass-element groups

were clearly distinguished. Regarding the vertical center of mass, it was assumed that M_V and M_P must be on the same level as M_T at Z_T.

On the basis of the fundamental assumptions, the mass reallocation parameter α ($0 < \alpha < 1$) was introduced as the ratio of M_V to M_T, i.e., $M_V = \alpha M_T$ and $M_P = (1 - \alpha)M_T$. Then, Eq. (4) can be expressed as Eqs. (5)-(6). Eq. (6) shows that the center of M_P is only dependent on the parameter α.

$$M_T \cdot \vec{c}_T = \alpha M_T \cdot \vec{c}_V + (1 - \alpha)M_T \cdot \vec{c}_P$$
$$= \alpha M_T \cdot (0,0,Z_T)^T + (1 - \alpha)M_T \cdot (X_P, Y_P, Z_T)^T \tag{5}$$

$$\therefore (X_P, Y_P)^T = \frac{1}{1 - \alpha}(X_T, Y_T)^T \tag{6}$$

where X_P and Y_P are the horizontal coordinate values for the center of M_P. Additionally, it makes sense that M_P was placed within the range of the decks because, in actuality,

(a) Mass allocation for the four jacket legs

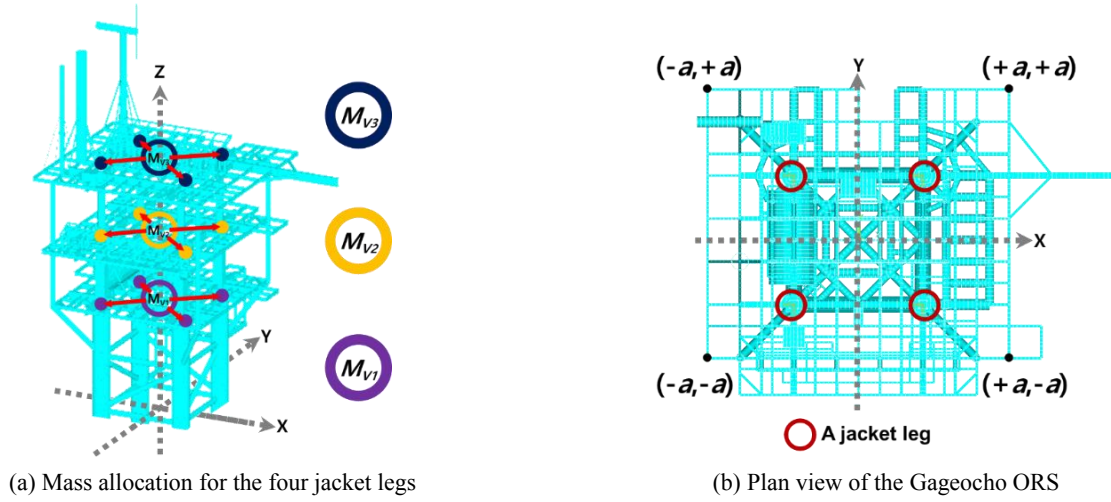(b) Plan view of the Gageocho ORS

Fig. 8 Mass allocation for the legs, and a plan view of the Gageocho jacket structure

all masses are within this range, as shown in Fig. 7(a). Thus, as shown in Fig. 8(b), X_P and Y_P were designed to be subject to the constraints presented in Eq. (7). Lastly, the parameter α for this model had the domain range defined in Eq. (8).

$$|X_P| \le a, \qquad |Y_P| \le a$$
$$\frac{1}{1-\alpha}|X_T| \le a, \quad \frac{1}{1-\alpha}|Y_T| \le a \qquad (7)$$
$$\alpha \le 1 - \frac{|X_T|}{a}, \quad \alpha \le 1 - \frac{|Y_T|}{a}$$

$$\therefore 0 < \alpha \le 1 - \frac{max(|X_T|, |Y_T|)}{a} \qquad (8)$$

3.5.1 Mass reallocation on the deck stories (M_P)

M_P was separated into M_{P1} and M_{P2} on the cellar and main decks, respectively. If M_P is applied to every three decks, the effect of mass momentum of equivalent mass on the dynamic characteristics can be represented by only M_P without M_V. In this case, M_V would become meaningless, and consequently M_P would be excessively large, thereby perturbing the dynamic modes and resulting in inaccurate model updates. More specifically, the local modes of the heavy masses applied to the slender and weak deck members could occur prior to the global modes of the structure, but this is not a realistic result. This is the reason why M_P was reallocated on the two decks (1st and 2nd floors) closer to the center of the equivalent mass.

The process of dividing M_P into M_{P1} and M_{P2}, and the equivalent mass momentum equilibrium, can be expressed as shown in Eqs. (9)-(10). These variables were transformed into a matrix, as shown in Eq. (11) to calculate the values for M_{P1} and M_{P2} (Eq. (12)).

$$M_P = M_{P1} + M_{P2} \qquad (9)$$

$$M_P \cdot Z_T = M_{P1} \cdot Z_1 + M_{P2} \cdot Z_2 \qquad (10)$$

$$\begin{bmatrix} 1 & 1 \\ Z_1 & Z_2 \end{bmatrix} \begin{vmatrix} M_{P1} \\ M_{P2} \end{vmatrix} = (1-\alpha)M_T \begin{vmatrix} 1 \\ Z_T \end{vmatrix} \qquad (11)$$

$$\therefore \begin{vmatrix} M_{P1} \\ M_{P2} \end{vmatrix} = (1-\alpha)\frac{M_T}{Z_2 - Z_1} \begin{vmatrix} Z_2 - Z_T \\ Z_T - Z_1 \end{vmatrix} \qquad (12)$$

3.5.2 Mass reallocation on the deck legs (M_V)

As was previously described for M_P, the equivalent mass and its center were applied to distribute M_V, as described by Eqs. (13)-(14).

$$M_V = M_{V1} + M_{V2} + M_{V2} \qquad (13)$$

$$M_V \cdot Z_T = M_{V1} \cdot Z_1 + M_{V2} \cdot Z_2 + M_{V3} \cdot Z_3 \qquad (14)$$

Similar to the method for defining the parameter α, the ratio of M_{V1} to M_V is defined as the parameter β ($0 < \beta < 1$), as shown in Eq. (15). Subsequently, Eqs. (13)-(14) can be obtained as the function of M_{V2} and M_{V3} by substituting M_{V1} with $\beta \cdot M_V$ in Eq. (15) to yield the matrix shown in Eq. (16).

$$M_{V1} = \beta M_V \qquad (15)$$

$$\begin{bmatrix} 1 & 1 \\ Z_2 & Z_3 \end{bmatrix} \begin{vmatrix} M_{V2} \\ M_{V3} \end{vmatrix} = M_V \begin{vmatrix} 1 - \beta \\ Z_T - \beta Z_1 \end{vmatrix} \qquad (16)$$

$$\therefore \begin{vmatrix} M_{V2} \\ M_{V3} \end{vmatrix} = \frac{M_V}{Z_3 - Z_2} \begin{vmatrix} Z_3 - Z_T - \beta(Z_3 - Z_1) \\ Z_T - Z_2 + \beta(Z_2 - Z_1) \end{vmatrix} \qquad (17)$$

It is certain that M_{V2} and M_{V3} cannot be negative, so the range of β can be obtained as shown in Eq. (18); then, M_{V1}, M_{V2}, and M_{V3} can be formulated by replacing M_V with $\alpha \cdot M_T$ and utilizing α, β, and M_T as shown in Eqs. (19)-(20).

$$\frac{Z_2 - Z_T}{Z_2 - Z_1} \le \beta \le \frac{Z_3 - Z_T}{Z_3 - Z_1} \qquad (18)$$

$$M_{V1} = \alpha \beta M_T \qquad (19)$$

$$\begin{vmatrix} M_{V2} \\ M_{V3} \end{vmatrix} = \frac{\alpha M_T}{Z_3 - Z_2} \begin{vmatrix} Z_3 - Z_T - \beta(Z_3 - Z_1) \\ Z_T - Z_2 + \beta(Z_2 - Z_1) \end{vmatrix} \qquad (20)$$

As a result of this formulation method, the natural frequency of the i-th mode, f^i, in the objective function of Model 4 is a function of the mass reallocation parameters α and β, as well as the elastic moduli of the steel and concrete. Therefore, the four parameters are updating parameters.

3.6 Model 5: reallocation of masses on lower and upper jacket legs and deck nodes

3.6.1 Grouping masses centered at 17 m above sea level

Although that the reallocation of the integrated mass to the platform seems reasonable by virtue of the fact that the centers of the equivalent masses are placed at the levels of the decks, considering the effects of the moment of inertia on the natural frequencies, there may be a limit to how precisely the model can reflect the conditions of the actual structure, because the masses are actually distributed throughout the entire structure, even far from the center, as shown in Fig. 7(a). For this reason, two different mass groupings that were centered at 17 m above sea level were set as M_U and M_L, corresponding to the upper and lower parts, respectively, before being independently reallocated as illustrated in Fig. 7(e).

Table 9 provides the values of M_U and M_L, in addition to the corresponding coordinates of the centers of mass, $\vec{c}_U$ and $\vec{c}_L$. Specifically, Z_U was 26.1841 m, so M_U was very close to the main deck, because the masses included in the lower part were excluded. The distance to the floor was only approximately 0.3 m, which does not seem very significant considering the fact that the spacing between the decks is 4.5 m. Thus, M_{UP}, corresponding to M_P of Model 4, was not shared between two decks, but only applied to the middle deck. Conversely, M_{UV} was determined exactly as described for M_V in Model 4. Therefore, the mass

reallocation parameters α and β shall be included in updating parameters, as the Model 4. One difference is that the approximation of M_{UP} causes the parameter β to be dependent on the parameter α; therefore, the search area for β was updated based on the results of α at each iteration.

3.6.2 Mass reallocation on the lower legs (M_L)

As listed in Table 9, M_L was 9.899 ton, meaning that approximately 10% of the integrated masses were distributed below 17 m. X_L and Y_L were 0.93 m and 2.85 m, respectively, so the center of M_L was much more eccentric than that of M_T. This is because X_L and Y_L were farther from the origin on the X-Y plane than X_T and Y_T. Therefore, how to accurately model the eccentricity was the main consideration for M_L. It should also be noted that there was no planar member in the lower parts, so M_L had to be shared among the four nodes on the legs.

For a more intuitive derivation of M_L, the Q-R plane coordinates were utilized instead of the global X-Y planar coordinates. The Q and R axes corresponded to a 45° rotation of the X and Y axes, respectively, about the positive Z axis, as shown in Fig. 9. As previously described, the conservation of M_L, and its center, before and after this reallocation was applied as described via Eqs. (21)-(23), and the reallocated nodal mass at any leg point on one of the four legs (e.g., M_Q^- at (-H,0)QR), can be expressed by creating a new reallocation parameter γ ($0 < \gamma < 1$), as shown in Eq. (24). These four equations can be written in matrix form (Eq. (25)); then, the amounts of the four nodal masses can be calculated by solving Eq. (26).

$$M_L = M_Q^+ + M_Q^- + M_R^+ + M_R^- \tag{21}$$

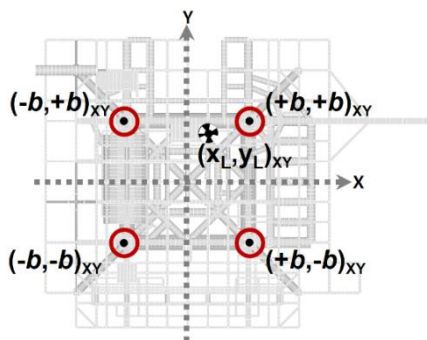$$M_L \cdot q_L = M_Q^+ \cdot H + M_Q^- \cdot (-H) \tag{22}$$

$$M_L \cdot r_L = M_R^+ \cdot H + M_R^- \cdot (-H) \tag{23}$$

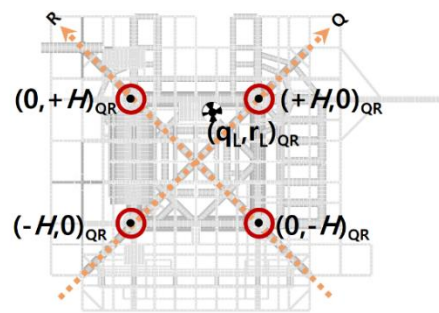$$\gamma \cdot M_L = M_Q^{-\prime} \tag{24}$$

$$\begin{bmatrix} 1 & 1 & 1 & 1 \\ H & -H & 0 & 0 \\ 0 & 0 & H & -H \\ 0 & 1 & 0 & 0 \end{bmatrix} \begin{vmatrix} M_Q^+ \\ M_Q^- \\ M_R^+ \\ M_R^- \end{vmatrix} = M_L \begin{vmatrix} 1 \\ q_L \\ r_L \\ \gamma \end{vmatrix} \tag{25}$$

Table 9 Equivalent masses and their locations (Model 5)

	Mass [ton]	Center of mass ($\vec{c}_U$ & $\vec{c}_L$)		
		X [m]	Y [m]	Z [m]
M_U [ton]	80.592	-0.0697	0.5099	26.1841
M_L [ton]	9.899	0.9313	2.8451	8.7615

(a) X-Y plane view

(b) Q-R plane view

Fig. 9 Plan views of the Gageocho jacket structure on the X-Y and Q-R plane

$$\therefore \begin{vmatrix} M_Q^+ \\ M_Q^- \\ M_R^+ \\ M_R^- \end{vmatrix} = M_L \begin{bmatrix} 0 & \dfrac{1}{H} & 0 & 1 \\ 0 & 0 & 0 & 1 \\ \dfrac{1}{2} & -\dfrac{1}{2H} & \dfrac{1}{2H} & -1 \\ \dfrac{1}{2} & -\dfrac{1}{2H} & -\dfrac{1}{2H} & -1 \end{bmatrix} \begin{vmatrix} 1 \\ q_L \\ r_L \\ \gamma \end{vmatrix} \qquad (26)$$

Additionally, all elements comprising the vector on the right-hand side of Eq. (26) are positive. Note that, although M_Q^+ and M_Q^- are always mathematically positive under such conditions, the others can sometimes be negative. However, the mass has to be non-negative, and M_R^- is always less than M_R^+. Therefore, an appropriate condition for the non-negative nodal masses in this problem is a non-negative M_R^-. This can be expressed as shown in Eq. (27). Additionally, the feasible range of the parameter γ was determined to be as shown in Eq. (28).

$$M_R^- = M_L \left(\frac{1}{2} - \frac{q_L}{2H} - \frac{r_L}{2H} - \gamma \right) \geq 0 \qquad (27)$$

$$\therefore 0 < \gamma \leq \frac{1}{2}\left(1 - \frac{q_L + r_L}{H} \right) \qquad (28)$$

Consequently, the five parameters, i.e., the respective moduli of elasticity E_s and E_c of the steel and concrete, and three mass reallocation parameters (α, β, and γ), were taken as the updating parameters in this model.

4. Updating results and discussion

4.1 Results summary

Table 10 lists the lowest five natural frequencies, root mean square errors (RMSEs), and the objective function values of eight different models. Table 11 presents the values of the two types of elastic moduli that were applied in all models and the updated results of the two elastic moduli for steel and concrete obtained from different initial models.

Table 10 Comparative result summaries

	Natural frequencies [Hz]					RMSE [%]	Objective function
Mode	1	2	3	4	5		
Measurement	1.790	1.827	2.652	5.599	5.694	-	-
Modified model	2.061	2.065	2.999	6.472	6.579	14.524	-
(Error [%])	15.14	13.03	13.08	15.59	15.54		
Model 1_Initial	1.843	1.845	2.283	4.109	5.146	14.175	0.17518
(Error [%])	2.961	1.007	-13.910	-26.621	-9.628		
Model 1	1.827	1.829	2.385	4.133	5.308	12.943	0.08680
(Error [%])	2.041	0.120	-10.08	-26.19	-6.772		
Model 2_Initial	2.119	2.124	5.919	6.013	6.368	56.516	0.90761
(Error [%])	18.380	16.267	123.179	7.398	11.832		
Model 2	1.634	1.639	4.070	4.955	5.329	25.358	0.30127
(Error [%])	-8.734	-10.27	53.48	-11.50	-6.416		
Model 3	1.596	1.984	2.736	5.263	5.306	7.530	0.14091
(Error [%])	-10.815	8.596	3.184	-6.002	-6.820		
Model 4_Initial	1.904	1.906	2.649	5.658	5.739	3.491	0.07721
(Error [%])	6.346	4.346	-0.128	1.056	0.790		
Model 4	1.807	1.810	2.653	5.617	5.644	0.736	0.01372
(Error [%])	0.962	-0.950	0.032	0.324	-0.880		
Model 5	1.807	1.809	2.654	5.586	5.685	0.631	0.01384
(Error [%])	0.973	-0.981	0.066	-0.232	-0.167		

Table 11 Elastic moduli E_c and E_s, corresponding to the updated results for each model in Table 8

Model	Modified model	Optimum values				
	Model 1&2_Initial	Model 1	Model 2	Model 3	Model 4	Model 5
E_c [GPa]	27.7	0.000	17202055	0.000	8.010	6.084
E_s [GPa]	200	234.612	70.052	171.310	201.107	215.407

4.2 Modified model

In general, this model is the preliminary FE model that has been revised to consider the corroded areas, and the concrete and steel piles in the four jacket legs. Regarding the natural frequencies obtained via the preliminary FE model, although the errors of the preliminary model (relative to the measured results) were larger than approximately 15% for all modes, the errors of the modified model were less than approximately 15% for every mode. The RMSE values also decreased from approximately 17.98% to 14.52%. In particular, the errors for lower modes, which were considerably larger than those for the higher modes in the preliminary FE model, decreased by nearly 6%.

4.3 Distributed masses: Model 1

The modified FE model was revised by considering all nodal masses. Initially, the two types of elastic moduli in the preliminary model were identical to those in the modified model, as given in Table 11; the results are listed in Table 10 as Model 1_Initial. For the modified model, the first two natural frequencies were significantly lower and relatively similar to the measured values. This can be considered to be a result of modeling the originally disregarded masses in the modified FE model. However, the RMSE only decreased by approximately 0.4% because the error of the 4th natural frequency increased.

The optimal values of the elastic moduli of the concrete and steel material were updated based on the Model 1_Initial value; the optimal E_c and E_s values, and their corresponding resultant natural frequencies, are summarized in Tables 7-8 (Model 1). It can be ascertained that the errors in Table 10 decreased by approximately 1~3% relative to the Model 1_Initial results. Although this can be attributed to the effect of optimization, the updated FE model does not seem to accurately represent the actual structure for several reasons. The first reason is that the errors for the 3rd to 5th modes were relatively large, and, particularly, the 4th natural frequency error reached 25%. Secondly, the RMSE of approximately 12.94% for Model 1 is not sufficient to ensure agreement with the measured data. Lastly, not only was the optimized E_c less than 1 MPa, which is too small, even considering its uncertainty, but the optimized E_s was also significantly larger than expected because the optimum value exceeded the mean (i.e., the design target value of the steel) by almost +2.83 standard deviation.

4.4 Equivalent nodal mass: Model 2 and Model 3

Regarding Models 2 and 3, the overall results, including those for the natural frequency errors, RMSEs, and optimum values of E_c and E_s, prove that these models are inadequate. This is especially evidenced by the optimal moduli of elasticity results. Specifically, the values for both types of materials were impossibly large. The reason for this is that the equivalent mass was modeled as one nodal mass at the center of mass.

Regarding Model 2, the initial model and design values for the elastic moduli are presented as Model 2_Initial, and

its natural frequencies are listed in Table 10. As compared to Model 1_Initial, every natural frequency increased by at least 15%; particularly, the 3rd natural frequency increased by nearly 160%. This means that the stiffness significantly increased, mainly affecting the torsional as well as bending behavior of the structure. The primary cause of this was the rigid connections to the equivalent mass. The connections rigidly linked four jacket legs to one another through the mass near the free end, and their effects overwhelmed the effect of the equivalent mass. Thus, the main problem became how to compensate for the influence of the rigid connections, but not the equivalent mass.

In this regard, the optimization process converged in the direction in which the effective length of the dynamic response of the structure decreased as a result of the elasticity of the concrete substantially increasing, as can be seen in Table 11. This resulted in all concrete components becoming too stiff to move; therefore, the height of the only movable parts above the concrete column became the effective dynamic length. The mode shapes for Model 2, as described in Fig. 10, also supports this hypothesis. As the concrete components stiffened, the steel materials became very compliant to compensate for the increasing stiffness brought about by the rigid connections and rigid concrete. This is because the objective function, i.e., the weighted RMSE, drove the convergence process to mainly controlling the bending stiffness, which consequently reduced the errors of four modes, i.e., excluding the 3rd torsional mode. Although the effects of such a convergence process caused all of the natural frequencies to decrease by at least 15% relative to the Model 2_Initial results, its RMSE was still larger than that for Model 1, Model 1_Initial, and the modified model. The reason for this is that the effects of the rigid connections on the torsional mode were more significant on other bending modes, and that the bending and torsional stiffness were differently affected by those parameters.

Model 3 was a trial to overcome such the shortcomings of Model 2, so 4 axial springs were applied instead of the
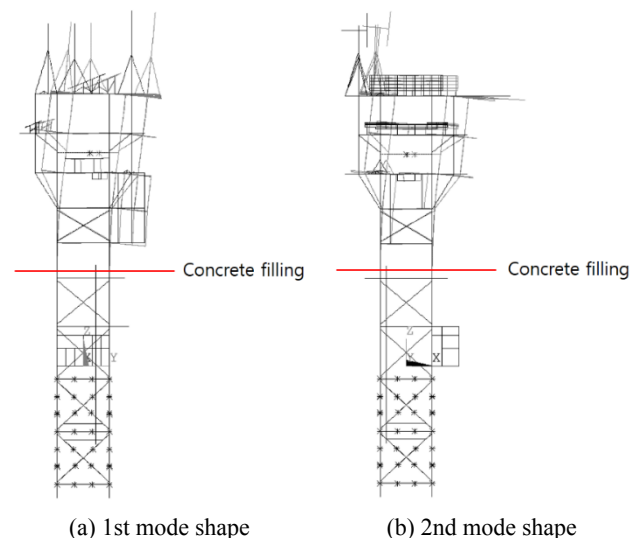

(a) 1st mode shape   (b) 2nd mode shape

Fig. 10 Mode shapes for Model 2, overlapped with their corresponding non-deformed shapes (auto-scaled)

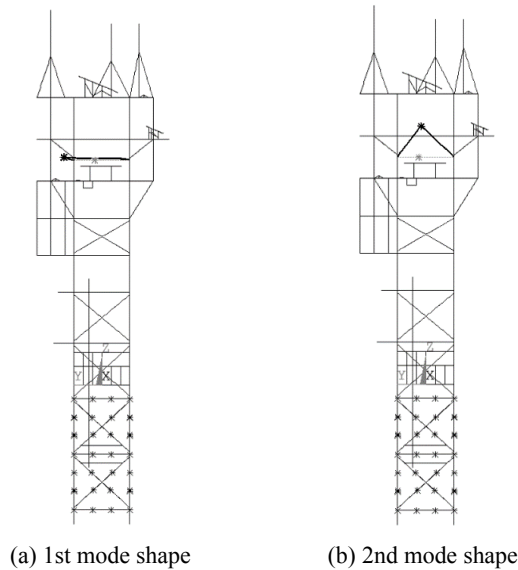(a) 1st mode shape   (b) 2nd mode shape

Fig. 11 Mode shapes for Model 3, overlapped with their
corresponding non-deformed shapes (auto-scaled)

rigid connection. In this case, however, local motions of the equivalent nodal mass are fairly likely to occur prior to the global behavior of the entire structure. In fact, the nodal mass rather separately vibrates with its own mass and stiffness as illustrated in Fig. 11, like seismic dampers for earthquake-proof, such as a tuned mass damper (TMD), although the motion is not perfectly independent with the behavior of the whole structure. For this reason, 3rd to 7th eigen frequencies of Model 3 corresponding to 1st to 5th natural frequencies of the jacket were used.

In the actual structure, the horizontal eccentricity seen in the measured natural frequencies would be attributed to distribution of mases under the assumption that there is no damage on the jacket. On Model 3, however, the stiffness of the virtual connections (S_1 to S_4 on Table 8) would have mainly influence on the eccentric behavior of Model 3, not only the equivalent nodal mass. For instance, even if the natural frequencies be well matched with each other, mode shapes, more specifically, the strong and weak axes may be different with the real Gageocho ORS; fortunately, such the issue did not happen in the optimal Model 3, though. Therefore, something different manner capable of evaluating the agreement of mode shapes, such as modal assurance criterion (MAC), would be required for this case.

4.5 Mass reallocation method:
Model 4 and Model 5

As shown in Table 10, all of the errors for the 1st to 5th modes were significantly reduced, and in the cases of Models 4 and 5, the errors were reduced to less than 1%. In particular, the errors corresponding to the 3rd natural frequency substantially decreased to less than 0.1%. It is noteworthy that that the accuracy of the 3rd mode, i.e., a torsional mode, may be an important factor that affects the ability of the model to precisely update the preliminary model. The rationale behind this is that there are no slight differences, depending on the X- and Y-axes, between the

1st and 2nd and 4th and 5th measured natural frequencies, and that they would be predominantly attributable to the eccentricity of the masses. This would limit the amount that the overall error could be reduced for all modes, including the two 1st-bending and two 2nd-bending natural frequencies, if the effect of the eccentric mass on the horizontal plane is not properly represented. Therefore, the 1st torsional mode can be considered as a direct parameter to evaluate the accuracy of the model updating in this case.

The optimized elastic modulus values are considered to be more suitable than the previously determined optimized values. The intuitive criterion for this is the optimization of the elastic modulus of the steel. This is because the properties of steel are generally easier to determine than those of concrete due to its uncertainty in curing process. It is known that the modulus of elasticity of steel is typically within the range of approximately 200–215 GPa, and the COV is considered as less than 0.06 (Hess *et al.* 2002). Considering this, the two optimized values of 201.11 GPa and 215.41 GPa (Table 11) for Models 4 and 5, respectively, are practical within one standard deviation from the initial value (i.e., design value). Therefore, these values verify the accuracy of Models 4 and 5, indicating that the steel structure would not incur any serious damage. Consequently, all of the concrete would remain in the jacket legs and not leak out into the sea. However, the optimized moduli of elasticity for Models 4 and 5 were less than one-third of the design value. Therefore, under the assumption that leakage did not affect the mass or density, the most reasonable reason for the lower moduli of elasticity is improper concrete curing.

Regarding the reallocated masses, Table 12 shows the results for M_V, M_P, and M_L (M_Q^+, M_Q^-, M_R^+, M_R^-). The masses of 66.74 and 23.76 ton were reallocated to M_V and M_P, respectively, in the case of Model 4. This means that approximately 26.25% of the equivalent mass contributes to the horizontal eccentricity of the dynamic response. This is considered to be an advantage, as it is possible to precisely determine the amount of mass that contributes to the eccentric dynamic properties. However, it is not easy to intuitively interpret the eccentric portion of the equivalent mass in Model 5 because of M_L. Hence, the difference between the opposing masses, $|M_Q^+ - M_Q^-|$ and $|M_R^+ - M_R^-|$, were regarded as the effective eccentric mass in this study, in consideration of the relationships between the center of mass and the masses and moment arms. Based on this, the eccentric portion of the equivalent mass in Model 5 was determined to be approximately 21.785 ton, which is slightly less than that in Model 4. The reason for this is that the eccentric mass can be distributed along height of a structure, so Model 5 is able to model this more precisely

Table 12 Reallocated masses of Model 4 and Model 5

	M_V	M_P	M_Q^+	M_Q^-	M_R^+	M_R^-
Model 4 [ton]	66.735	23.756	-	-	-	-
Model 5 [ton]	61.880	18.712	6.231	3.413	0.000	0.256

than Model 4. This is a merit of Model 5.

Lastly, Table 13 and Fig. 12 presents the masses with respect to the vertical height, and it also provides a comparison, showing that the simulated masses overlapped with the original mass distribution. In Model 4, most of the equivalent mass was reallocated to on the main and cellar decks. This is because M_P was only shared between the two decks. This allocation method did not yield results that were well-matched with the original mass distribution. Conversely, most of the mass was concentrated on the main deck in the case of Model 5. The reason for this is that the upper masses were nearly symmetrically distributed about the main deck. Consequently, the tendency of mass reallocation in Model 5 was better representative of the actual mass ratio for the three decks.

These results inform that model updating of a jacket-type offshore structure has a unique characteristic dissimilar with updating an FE model of other infrastructures such as general buildings and bridges. While it is general to control the density of the materials to model the others because they are dominantly affected by the mass of themselves, it is required to thoroughly model the influence of the masses of non-structural components. Moreover, it should reflect the

higher effect induced by the locations of the masses as well as just the total amount of them. This is because the jacket-ype offshore structure is a space lattice so non-structural masses are relatively significant compared to the other structures. Furthermore, another reason is that the bulk of the non-structural components are usually located on the topside platform, i.e., almost free-end where the structure responds most sensitively for mass. Therefore, it would be possible to use this technique to modeling other lattice-type offshore structures, for example, a compliant tower and a jack-up rig. On top of that, it would also be effectively available to identify and update a significant change of mass. The sudden variation of the mass usually happens after loading, unloading (or offloading) in the offshore structures whereas such the change does not occur in the case of general onshore infrastructures.

To sum up, it was performed that the five FE models for the Gageocho ORS were made and independently updated from beginning to end. As the final outcome, the most adequate model was determined and it was shown that the mass reallocation method proposed in this study was effective to generate a reliable FE model to an actual offshore jacket structure. Like this procedure, some techniques used for SHM start an FE model updating for a structural system from several different initial FE models under various conditions, and multi-model updating method (Link and Weiland 2009, Link *et al*. 2008) is one of them. It was studied that, to be more specific, when a model updating is used for damage detection to a structural system, the method that the intact model and the damaged model are simultaneously modified with influencing each other could allow finding the unique solution to the problem. For a future study, it can be applied to identify the structural integrity of the Gageocho ORS to assure its structural safety for maintenance.

Table 13 Masses according to vertical height

	Model 4	Model 5
Roof [ton]	1.505	5.591
Main [ton]	42.799	63.752
Cellar [ton]	46.187	11.249
Lower legs [ton]	0	9.899
Total [ton]	90.491	90.491
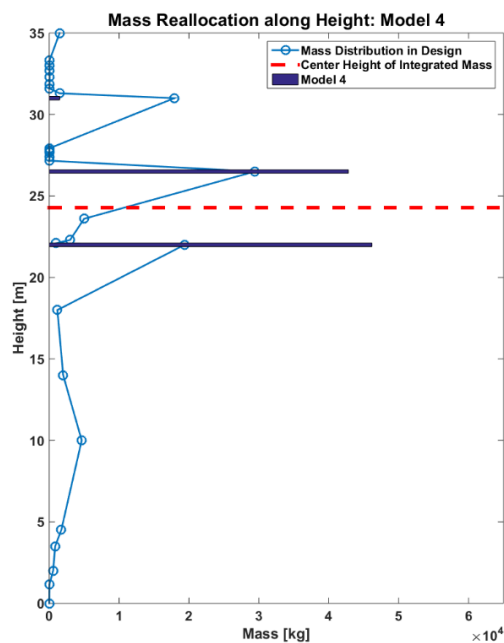
(a) Model 4
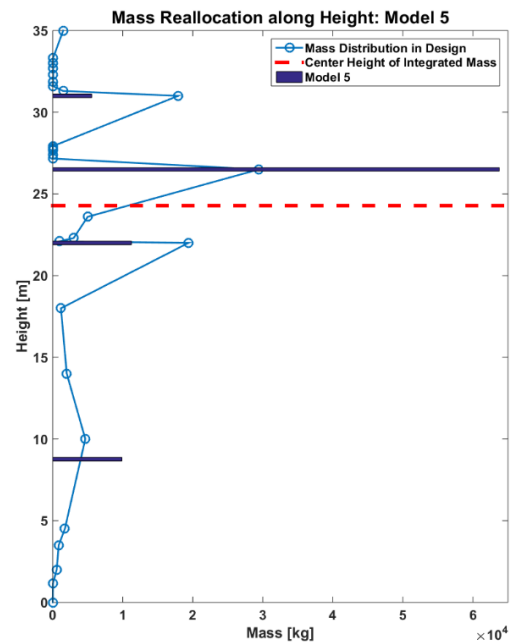
(b) Model 5

Fig. 12 Mass reallocation along height

5. Conclusions

In this study, FE model updating was carried out for the Gageocho ORS, which is one of jacket-type offshore structures and was retrofitted after incurring severe damage as a result of Typhoon Muifa in 2011, on the basis of its measured dynamic characteristics; the following summary were made:

(1) The consideration of what was done in the actual construction is of great importance when building an FE model based on the design-drawing since the natural frequencies of the only design drawing-based preliminary FE model did not match well with those obtained via measurements; the primary causes were classified as modeling and construction errors; the extra masses and concrete fillings disregarded in the preliminary model were considered as the main parameters to be updated.

(2) Three different initial FE models were established to update the elastic moduli of steel and concrete and the location and spring constants for modeling integrated mass; then, which model is most suitable for model updating was investigated by evaluating their updated parameters, i.e., the elastic moduli of the steel and concrete components.

(3) It was ineffective that all the respective non-structural masses were individually modeled as Model 1 while simplistically modeling them as the only integrated nodal mass as Model 2 and 3 caused another problem about how to define and deals with the connection between the nodal mass and the main structure; The common limitation of Model 1, 2, and 3 was that the elastic moduli converged into abnormal values, i.e., too small or too large, as their natural frequencies got closer to the measured values during iterations.

Based on the above-mentioned results, i.e., the calculated natural frequencies don't converge to the identified natural frequencies, the mass reallocation method is newly proposed in this study to rationally model the effects of the masses for many number of facilities. Two mass reallocation models were considered as Model 4 and Model 5. And the following conclusions were obtained:

(1) The mass reallocation method did not result in any connection problems and was less time-consuming than modeling all of the nodal masses. The updated FE models that were based on the initial Models 4 and 5 yielded very small errors, i.e., less than 1% for all the five modes, and the updated values of elastic modulus of steel were also reasonable. This accuracy was credited to the ability of the models to effectively represent the effects of mass eccentricity, as well as the characteristics of the global dynamic response according to the height of masses.

(2) Employing the mass reallocation method enabled quantification of the amount of mass that contributed to the dynamic eccentricity, thereby demonstrating the importance of precise identifica-tion of the eccentricity in model updating based on structural dynamic properties.

This research is worthy of notice from the point of view that the results from the full-scale measurement data in real operation for a jacket-type offshore structure have not been widely available from existing references in the public domain. However, they are one of the most common structure types commonly used in an offshore oil and gas industry. On top of this, a new approach was proposed to model non-structural mass components efficiently, which would have a significant effect on the dynamic properties of the entire structure. In the cases of the offshore structure with many non-structural components such as facilities and equipment were not negligible compared to the weight of the structure itself as well as were difficult to be treated one by one, the proposed method would be a great solution to perform the modeling task. Consequently, it is expected that this research would make a significant contribution to the structural integrity evaluation of decrepit offshore plants based on measurement in the future.

Acknowledgments

References

Ansys Inc. (2017), Ansys Mechanical Advanced Parametric Design Language v17.1.

Baji, H. (2014), "The effect of uncertainty in material properties and model error on the reliability of strength and ductility of reinforced concrete members", Ph.D. Dissertation, University of Queensland, Brisbane, Australia.

Bayraktar, A., Sevim, B. and Altunişika, A.C. (2011), "Finite element model updating effects on nonlinear seismic response of arch dam-reservoir-foundation systems", *Finite Elem. Anal. Des.*, **47**(2), 85-97. https://doi.org/10.1016/j.finel.2010.09.005

Boscato, G. and Russo, S. (2015), "Global sensitivity-based model updating for heritage structures", *Comput.-Aided Civil Infrastruct. Eng.*, **30**(8), 620-635. https://doi.org/10.1111/mice.12138

Cremona, C. and Santos, J. (2018), "Structural health monitoring as a big-data problem", *Struct. Eng. Int.*, **28**(3), 243-254. https://doi.org/10.1080/10168664.2018.1461536

Deng, L. and Cai, C.S. (2010), "Bridge model updating using response surface method and genetic algorithm", *J. Bridge Eng.*, **15**(5), 553-564. https://doi.org/10.1061/(ASCE)BE.1943-5592.0000092

Engineering Dynamics, Inc. (1995), SACS USER'S MANUAL Release 4.

Fang, S.E. and Perera, R. (2009), "A response surface methodology based damage identification technique", *Smart Mater. Struct.*, **18**(6), 065009. https://doi.org/10.1088/0964-1726/18/6/065009

Foti, D., Diaferio, M., Giannoccaro, N.I. and Mongelli, M. (2012), "Ambient vibration testing, dynamic identification and model updating of a historic tower", *NDT&E Int.*, **47**, 88-95. https://doi.org/10.1016/j.ndteint.2011.11.009

Fritzen, C.P., Klinkov, M., Kraemerbbs, P. and Koranyi, B. (2013), *Vibration-Based Damage Diagnosis and Monitoring of External Loads*, W. Ostachowicz and J.A. Güemes (eds.), New Trends in Structural Health Monitoring, January.

Han, J.P. and Luo, Y.P. (2013), "Static and dynamic finite element model updating of a rigid frame-continuous girders bridge based on response surface method", *Adv. Mater. Res.*, **639-640**, 992-997. https://doi.org/10.4028/www.scientific.net/AMR.639-640.992

Hess, P.E., Bruchman, D., Assakkaf, I.A. and Ayyub, B.M. (2002), "Uncertainties in material and geometric strength and load variables", *Naval Engr. J.*, **114**(2), 139-166. https://doi.org/10.1111/j.1559-3584.2002.tb00128.x

Hosseinlou, F. and Mojtahedi, A. (2016), "FEM Updating for Offshore Jacket Structures Using measured Incomplete Modal Data", *Int. J. Maritime Technol.*, **5**, 1-11.

Hosseinlou, F., Mojtahedi, A. and Yaghin, M.A.L. (2017), "Developing a SIM strategy for offshore jacket platforms based on the FE model updating and a novel simplified method", *Ocean Eng.*, **145**, 158-176. https://doi.org/10.1016/j.oceaneng.2017.08.013

Jacquenot, G. (2009), Example of convergence of a direct search method on Broyden function. https://commons.wikimedia.org/wiki/File:Direct_search_BROY DEN.gif (Accessed 11 August 2019)

Kim, D.H., Shim, J.S. and Min, I.K. (2006), "Dynamic response of Ieodo ocean research station", *J. Coastal Ocean Engr.*, **18**(1), 53-62. [In Korean]

Kim, W., Yi, J.H., Min, I.K. and Shim, J.S. (2017), "Estimation of dynamic characteristics of Gageocho Ocean Research Station using long-term measurement data", *J. Coastal Disaster Prev.*, **4**(5), 263-270. [In Korean]

Kim, B., Kim, C. and Yi, J.H. (2019), "Model Updating for Gageocho Ocean Research Station Structure Using Structural Dynamic Characteristics", *J. Coastal Disast. Prev.*, **6**(5), 103-110. [In Korean]

Lei, Y., Wang, H.F. and Shen, W.A. (2012), "Update the finite element model of Canton Tower based on direct matrix updating with incomplete modal data", *Smart Struct. Syst., Int. J.*, **10**(4-5), 471-483. https://doi.org/10.12989/sss.2012.10.4_5.471

Li, Y. and Li, H. (2011), "Boundary Updating of Offshore Jacket Structures Based on Measured Modal Frequencies", *Proceedings of the 21st (2011) International Offshore and Polar Engineering Conference*, Hawaii, USA, June, pp. 219-225.

Link, M. and Weiland, M. (2009), "Damage identification by multi-model updating in the modal and in the time domain", *Mech. Syst. Signal Process.*, **23**(6), 1734-1746. https://doi.org/10.1016/j.ymssp.2008.11.009

Link, M., Weiland, M., and Seckert, Th. (2008), "Computational model updating for damage identification in the time domain", *Proceedings of ISMA 2008: International Conference on Noise and Vibration Engineering*, Leuven, Belgium, September, pp. 3293-3305.

Mottershead, J.E., Link, M. and Friswell, M.I. (2011), "The sensitivity method in finite element model updating: A tutorial", *Mech. Syst. Signal Processing*, **25**(7), 2275-2296. https://doi.org/10.1016/j.ymssp.2010.10.012

Ni, Y.Q., Xia, Y., Lin, W., Chen, W.H. and Ko, J.M. (2012), "SHM benchmark for high-rise structures: a reduced-order finite element model and field measurement data", *Smart Struct. Syst., Int. J.*, **10**(4-5), 412-426. https://doi.org/10.12989/sss.2012.10.4_5.411

Oil & Gas UK. (2012), "The Decommissioning of steel piled jackets in the northern sea region", The United Kingdom Offshore Oil and Gas Industry Association Limited trading as Oil & Gas UK.

Ren, W.X. and Chen, H.B. (2010), "Finite element model updating in structural dynamics by using the response surface method", *Eng. Struct.*, **32**(8), 2455-2465. https://doi.org/10.1016/j.engstruct.2010.04.019

Sehgal, S. and Kumar, H. (2015), "Structural dynamic model updating techniques: A state of the art review", *Arch. Computat. Methods Eng.*, **23**(3), 515-533. https://doi.org/10.1007/s11831-015-9150-3

Shim, J.S., Chun, I.S., Min, I.K. and Kim, S.S. (2015), "A study on damage recovery for Gageocho ocean research station", *KSCE 2015 Convention & Civil Expo*, Gunsan, South Korea, October. [In Korean]

Teughels, A. and Roeck, G.D. (2004), "Structural damage identification of the highway bride Z24 by FE model updating", *J. Sound Vib.*, **278**(3), 589-610. https://doi.org/10.1016/j.jsv.2003.10.041

The MathWorks, Inc. (2015), MATLAB and Global Optimization Toolbox Release 2015a, Natick, MA, USA.

Woo, C. and Sin, J. (2012), "Precision Safety Diagnosis and Disaster Recovery Design of Gageocho Ocean Research Station", Report No. BSPE98689-10169-7, Korean Ocean Research & Development Institute. [In Korean]

Yi, J.H., Park, J.S., Han, S.H. and Lee, K.S. (2013), "Modal identification of a jacket-type offshore structure using dynamic tilt response and investigation of tidal effects on modal properties", *Eng. Struct.*, **49**, 767-781. https://doi.org/10.1016/j.engstruct.2012.12.015

Yu, E. and Chung, L. (2012), "Seismic damage detection of a reinforced concrete structure by finite element model updating", *Smart Struct. Syst., Int. J.*, **9**(3), 253-271. https://doi.org/10.12989/sss.2012.9.3.253

Zhou, L., Wang, L., Chen, L. and Ou, J. (2016), "Structural finite element model updating by using response surfaces and radial basis functions", *Adv. Struct. Eng.*, **19**(9), 1446-1462. https://doi.org/10.1177/1369433216643876

HJ